Two-Dimensional Crystallization of Microspheres by a Coplanar AC Electric Field

Simon O. Lumsdon,[†] Eric W. Kaler,[‡] and Orlin D. Velev*,[§]

DuPont Central Research & Development, Experimental Station, Wilmington, Delaware 19880, Department of Chemical Engineering, University of Delaware, Newark, Delaware 19716, and Department of Chemical Engineering, North Carolina State University, Raleigh, North Carolina 27695

Received September 28, 2003. In Final Form: January 2, 2004

The particle−field and particle−particle interactions induced by alternating electric fields can be conveniently used for on-chip assembly of colloidal crystals. Two coplanar electrodes with a millimeter-sized gap between them are used here to assemble two-dimensional crystals from suspensions of either latex or silica microspheres. When an AC voltage is applied, the particles accumulate and crystallize on the surface between the electrodes. Light diffraction and microscopic observations demonstrate that the hexagonal crystal is always oriented with one axis along the direction of the field. The particles disassemble when the field is turned off, and the process can be repeated many times. The diffraction patterns from all consecutively formed crystals are identical. This assembly is driven by forces that depend on the electric field gradient, and a model is proposed involving a combination of dielectrophoresis and induced dipole chaining. The organization of large two-dimensional crystals allows characterization of the electrostatic interactions in the particle ensembles. The process can be controlled via the field strength, the frequency, and the viscosity of the liquid media. It could be used to make rudimentary optical switches or to separate mixtures of particles of different sizes.

Introduction

The engineered assembly of colloidal particles can be used to create colloidal crystals that serve as precursors for advanced materials for photonics[1−5] and could be used in sensors, displays, and optical or electronic devices.[6−8] Colloidal crystal assembly can be effected by a variety of forces such as electrostatic repulsion and van der Waals attraction, hydrodynamic liquid drag,[7−10] and capillary forces acting on fluid surfaces.[9−13] In most situations, however, these forces do not readily provide the specific control and rapidity required for technological applications of particle assembly processes.

An efficient and convenient way to manipulate colloidal particles in suspension is to apply electrical fields from external electrodes. Processes driven by external fields can be rapid and precisely controlled. Electrophoretic forces make charged particles move in a constant (DC) field, and they have been widely studied and used.[14−18] However, particles can be even more efficiently manipulated by the use of alternating (AC) fields.[19−21] The application of an AC field with frequency ω across a suspension of colloidal particles leads to their polarization. The sign and magnitude of the resulting induced dipoles depend on the effective polarizability of the particles, which is given by the real part of the Clausius−Mossotti function, K:

$$\mathrm{Re}|\underline{K}| = \frac{\epsilon_2 - \epsilon_1}{\epsilon_2 + 2\epsilon_1} + \frac{3(\epsilon_1\sigma_2 - \epsilon_2\sigma_1)}{\tau_{MW}(\sigma_2 + 2\sigma_1)^2(1 + \omega^2\tau_{MW}{}^2)} \quad (1)$$

where ϵ_1 (and ϵ_2) and σ_1 (and σ_2) are the dielectric permittivity and conductivity of the media and the particles, respectively.[22] For dielectric particles, this function changes sign (i.e., the force changes from attractive to repulsive) at a crossover frequency of $\omega_C = (\tau_{MW})^{-1}$, where τ_{MW} is the Maxwell−Wagner charge relaxation time: $\tau_{MW} = (\epsilon_2 + \epsilon_1)/(\sigma_2 + 2\sigma_1)$. Such a frequency-dependent change of sign of the interactions is commonly observed with polymer microspheres in water[23−28] and allows a high degree of control of particle mobility.

* Corresponding author. E-mail: odvelev@unity.ncsu.edu.
[†] DuPont Central Research & Development.
[‡] University of Delaware.
[§] North Carolina State University.

(1) Joannopoulos, J. D. *Nature* **2001**, *414*, 257.
(2) Velev, O. D.; Kaler, E. W. *Adv. Mater.* **2000**, *12*, 531.
(3) Colvin, V. L. *MRS Bull.* **2001**, *26*, 637.
(4) Norris, D. J.; Vlasov, Y. A. *Adv. Mater.* **2001**, *13*, 371.
(5) Vlasov, Y. A.; Bo, X. Z.; Sturm, J. C.; Norris, D. J. *Nature* **2001**, *414*, 289.
(6) Holtz, J. H.; Asher, S. A. *Nature* **1997**, *389*, 829.
(7) Velev, O. D.; Lenhoff, A. M. *Curr. Opin. Colloid Interface Sci.* **2000**, *5*, 56.
(8) Jiang, P.; Bertone, J. F.; Hwang, K. S.; Colvin, V. L. *Chem. Mater.* **1999**, *11*, 2132.
(9) Denkov, N. D.; Velev, O. D.; Kralchevsky, P. A.; Ivanov, I. B.; Yoshimura, H.; Nagayama, K. *Langmuir* **1992**, *8*, 3183.
(10) Dimitrov, A. S.; Nagayama, K. *Langmuir* **1996**, *12*, 1303.
(11) Kralchevsky, P. A.; Denkov, N. D.; Paunov, V. N.; Velev, O. D.; Ivanov, I. B.; Yoshimura, H.; Nagayama, K. *J. Phys.: Condens. Matter* **1994**, *6*, A395.
(12) Kralchevsky, P. A.; Nagayama, K. *Adv. Colloid. Interface Sci.* **2000**, *85*, 145.
(13) Bowden, N.; Terfort, A.; Carbeck, J.; Whitesides, G. M. *Science* **1997**, *276*, 233.
(14) Trau, M.; Sankaran, S.; Saville, D. A.; Aksay, I. A. *Nature* **1995**, *374*, 437.
(15) Trau, M.; Saville, D. A.; Aksay, I. A. *Science* **1996**, *272*, 706.
(16) Bohmer, M. *Langmuir* **1996**, *12*, 5747.
(17) Hayward, R. C.; Saville, D. A.; Aksay, I. A. *Nature* **2000**, *404*, 56.
(18) Solomentsev, Y.; Bohmer, M.; Anderson, J. L. *Langmuir* **1997**, *13*, 6058.
(19) Gong, T.; Marr, D. W. M. *Langmuir* **2001**, *17*, 2301.
(20) Larsen, A. E.; Grier, D. G. *Phys. Rev. Lett.* **1996**, *76*, 3862.
(21) Richetti, P.; Prost, J.; Barois, P. *J. Phys. Lett.* (*Paris*) **1984**, *45*, 1137.
(22) Jones, T. B. *Electromechanics of Particles*; Cambridge University Press: Cambridge, 1995.
(23) Pethig, R. *Crit. Rev. Biotechnol.* **1996**, *16*, 331.
(24) Pethig, R.; Huang, Y. H.; Wang, X. B.; Burt, J. P. H. *J. Phys. D: Appl. Phys.* **1992**, *25*, 881.

10.1021/la035812y CCC: $27.50
Published on Web 02/14/2004

The dipoles of the polarized particles interact with the imposed electric fields. The resulting dielectrophoretic (DEP) force, F_{DEP}, depends on the field gradient, ∇E^2, and the radius of the particle, r:[22−28]

$$\vec{F}_{DEP} = 2\pi\epsilon_1 \mathrm{Re}|K(\omega)|r^3 \nabla {E_{rms}}^2 \quad (2)$$

The use of alternating voltage allows manipulation of virtually any type of particle in any type of media and has the advantage of permitting high field strengths without causing water electrolysis or electro-osmotic currents, either of which can disrupt particle ordering. For example, dielectrophoresis has been used as a tool for the assembly of composite particles,[26,28] microscopic biosensors,[29] and electrically functional microwires from gold nanoparticles.[30]

The dipoles induced in the particles of a suspension by either AC or DC fields also interact with each other, resulting in a "chaining" force, F_{chain}. This force depends on the field strength, E. A generalized expression for the force between adjacent polarized particles is

$$F_{chain} = -C\pi\epsilon_1 \mathrm{Re}|K(\omega)|^2 r^2 E^2 \quad (3)$$

where the coefficient C ranges from 3 to >1000 depending on the distance between the particles and the length of the particle chain.[22] Dipolar chaining has long been studied for application in electrorheological and magnetorheological fluids, which drastically increase their viscosity and become rigid when the particles adhere in the field.[31,32]

Electrical fields can be used to speed up the assembly of colloidal crystals. Both DC and AC fields have been used to drive the formation of two-dimensional (2D) and three-dimensional (3D) colloidal crystals between opposing parallel electrodes. Electrophoretic attraction of particles to surfaces has been used to speed the assembly of 3D crystals in order to make microsphere "opals".[33−35] The application of DC fields in the thin gap between conductive electrodes has been demonstrated to be a rapid and efficient way to assemble 2D crystals on surfaces.[14−18] The driving force bringing together the particles in these two-dimensional crystals has been experimentally and theoretically proven to be the electrohydrodynamic interaction of the flows around the microspheres, leading to attraction between the particles and their aggregation into ordered arrays.[16−18,36,37]

AC fields have also been used to modulate and align the structure of colloidal crystals. The most common examples

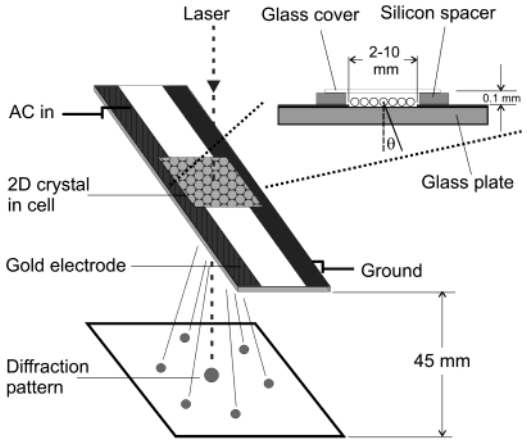

Figure 1. Schematics of the experimental arrangement and dimensions of the experimental cell.

are electrorheological fluids, where the particles commonly arrange into three-dimensional body-centered tetragonal (bct) crystals,[38] and various stable and metastable crystalline phases have been reported in electrorheological suspensions of silica spheres.[39] The chaining effect has been used to induce annealing and large-scale orientation of colloidal crystals formed by conventional sedimentation.[40] The electrophoretic mobility at frequencies below 100 Hz can cause particle compression and long-range crystallization in highly deionized systems.[20] Alternatively, when the opposing electrodes are only a few particle diameters away from each other, so the spheres are confined in a film, the repulsion between the parallel dipoles induced in the particles leads to long-range repulsive forces and 2D crystallization.[19,41] AC fields have recently been used to assemble 3D colloidal crystals.[42]

Here, we report the joint use of the dipole−field (DEP) and dipole−dipole (chaining) interactions for the assembly of colloidal microspheres into one-dimensional (1D) and two-dimensional structures on the glass surface of a thin cell. The geometry of this cell is unique in that it has both electrodes deposited on the same surface with a large gap between them.[43] Thus, the electric field is parallel, and the gradient of the field is normal, to the surface.

Experimental Section

Materials. Deionized water with a resistivity of 18.2 MΩ cm was obtained from a Millipore Milli-Q Plus water purification system. NaCl (99+%) and glycerol (99+%) were purchased from Fisher Scientific (PA). Surfactant-free polystyrene microspheres of diameters in the range of 0.7−1.4 μm were colloidally stabilized by surface sulfate groups and were purchased as aqueous dispersions from Interfacial Dynamics Corp. (OR). The 5 wt % surfactant-free aqueous dispersions of silica microspheres were purchased from Bangs Laboratories (IN).

Experimental Cell and Setup. A schematic illustration of the setup is shown in Figure 1. Particle assembly takes place inside a thin layer of suspension encapsulated above a microscope glass slide (25 × 75 mm plain microslide, VWR Scientific, PA). Two planar gold electrodes were deposited on the glass slides by

(25) Müller, T.; Gerardino, A.; Schnelle, T.; Shirley, S. G.; Bordoni, F.; DeGasperis, G.; Leoni, R.; Fuhr, G. *J. Phys. D: Appl. Phys.* **1996**, *29*, 340.
(26) Fuhr, G.; Müller, T.; Schnelle, T.; Hagedorn, R.; Voigt, A.; Fiedler, S.; Arnold, W. M.; Zimmermann, U.; Wagner, B.; Heuberger, A. *Naturwissenschaften* **1994**, *81*, 528.
(27) Pohl, H. A. *Dielectrophoresis*; Cambridge University Press: Cambridge, 1978.
(28) Morgan, H.; Green, N. G. *AC Electrokinetics*: *Colloids and Nanoparticles*; Research Studies Press: Baldock, U.K., 2003.
(29) Velev, O. D.; Kaler, E. W. *Langmuir* **1999**, *15*, 3693.
(30) Hermanson, K. D.; Lumsdon, S. O.; Williams, J. P.; Kaler, E. W.; Velev, O. D. *Science* **2001**, *294*, 1082.
(31) Gast, A. P.; Zukoski, C. F. *Adv. Colloid Interface Sci.* **1989**, *30*, 153.
(32) Parthasarathy, M.; Klingenberg, D. J. *Mater. Sci. Eng., R* **1996**, *17*, 57.
(33) Giersig, M.; Mulvaney, P. *Langmuir* **1993**, *9*, 3408.
(34) Holgado, M.; Garcia-Santamaria, F.; Blanco, A.; Ibisate, M.; Cintas, A.; Miguez, H.; Serna, C. J.; Molpeceres, C.; Requena, J.; Mifsud, A.; Meseguer, F.; Lopez, C. *Langmuir* **1999**, *15*, 4701.
(35) Rogach, A. L.; Kotov, N. A.; Koktysh, D. S.; Ostrander, J. W.; Ragoisha, G. A. *Chem. Mater.* **2000**, *12*, 2721.
(36) Trau, M.; Saville, D. A.; Aksay, I. A. *Langmuir* **1997**, *13*, 6375.
(37) Sides, P. J. *Langmuir* **2001**, *17*, 5791.
(38) Martin, J. E.; Odinek, J.; Halsey, T. C.; Kamien, R. *Phys. Rev. E* **1998**, *57*, 756.
(39) Dassanayake, U.; Fraden, S.; van Blaaderen, A. J. *J. Chem. Phys.* **2000**, *112*, 3851.
(40) van Blaaderen, A. J.; Velikov, K. P.; Hoogenboom, J. P.; Vossen, D. L. J.; Yethiraj, A.; Dullens, R.; van Dillen, T.; Polman, A. *Photonic Crystals and Light Localization in the 21st Century*; Soukoulis, C. M., Ed.; Kluwer: Amsterdam, 2001.
(41) Gong, T.; Wu, D. T.; Marr, D. W. M. *Langmuir* **2002**, *18*, 10064.
(42) Gong, T.; Wu, D. T.; Marr, D. W. M. *Langmuir* **2003**, *19*, 5967.
(43) Lumsdon, S. O.; Kaler, E. W.; Williams, J. P.; Velev, O. D. *Appl. Phys. Lett.* **2003**, *82*, 949.

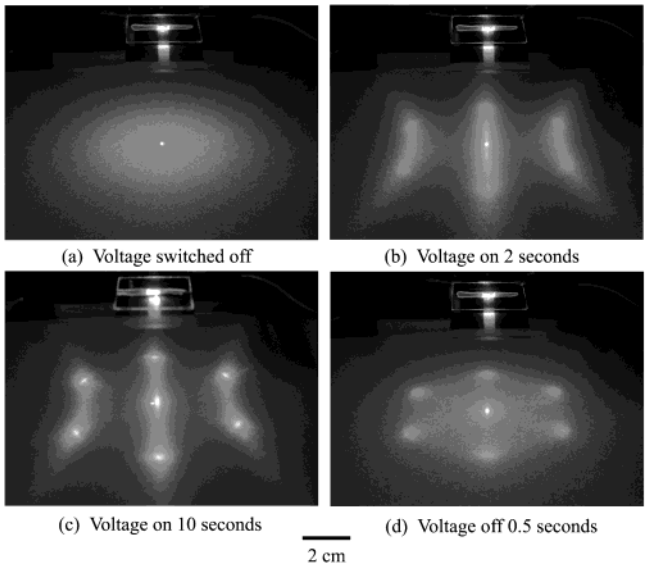

Figure 2. The diffraction patterns of a transmitted laser beam obtained as 1.0 μm latex particles crystallize, shown as a function of time since application of the electric field. (a) Before the field is applied, diffuse scattering indicates amorphous order. (b) Two seconds after turning the field on, the laser beam is diffracted into three parallel lines. (c) After 10 s, the laser beam is diffracted into six spots with hexagonal symmetry. (d) The diffraction pattern is lost shortly after the field is removed as the particles diffuse out of the array.

vapor deposition of layers of 10 nm of chromium followed by 100 nm of gold. The particle suspension was placed in the gap between the electrodes on the glass surface and was enclosed inside a hydrophobic spacer (PAP Pen, InnoGenex, CA) and covered with a microscope glass coverslip (25 × 25 mm micro cover glass, VWR Scientific). The characteristic dimensions of the experimental cell are given in the inset of Figure 1. The concentration of the particles inside the cell was adjusted with respect to the thickness, so when all of the particles from the cell volume were collected on the surface they formed a complete closely packed monolayer (e.g., 0.5 vol % for a suspension of 1 μm diameter spheres).

The alternating electric field was produced using a Beckmann FG3A function generator connected to a Burleigh model PZ-70 amplifier. Fields of intensities in the range of 40−100 V at a frequency of 200−20 000 Hz (typically 500 Hz) were used to assemble the crystals. The particles in the chamber were observed from above using an Olympus BH-2 optical microscope. The diffraction pattern of a He−Ne laser beam (Spectra-Physics, λ = 632.8 nm, beam diameter = 0.4 mm) was collected on a screen 45 mm below the glass slide. The diffraction patterns were recorded using a Sony Mavica digital camera.

Results and Discussion

Two-Dimensional Assembly under the Action of the AC Field. Three concurrent observations were carried out to characterize the assembly process. First, the diffraction pattern of a laser beam directed through the particle suspension provided information about the averaged structure of the particle ensemble. The particle dynamics and structure formed on field application were also directly observed by high-magnification microscopy. Finally, the overall optical properties of the arrays were evaluated by transmittance and reflectance of white monochromatic light.

Figure 2 shows the laser diffraction pattern obtained from 1 μm diameter polystyrene latex spheres as a function of the time since application of the electric field. Before the field is applied, the particles are randomly distributed through the volume of the cell due to Brownian motion and display only diffuse scattering (Figure 2a). Two seconds after applying the field, the laser beam is diffracted into three parallel lines that are perpendicular to the direction of the applied field (Figure 2b). This is an intermediate stage as the pattern evolves into a hexagonal array of six individual spots after approximately 10 s (Figure 2c). This spot array is indicative of diffraction from hexagonally close-packed spheres. The pattern is highly reproducible over the crystal area with the position of the six spots remaining the same no matter what area of the cell the laser is directed through. This proves that the crystal has continuous single-domain orientation throughout the whole area. In contrast, the multidomain 2D crystals deposited by conventional convective assembly[9,10] display a ring-line diffraction pattern when the beam size is larger than the characteristic domain size or six spots at different radial positions if scanned with a beam of very small diameter.[44] After the electric field is removed, the diffuse scattering pattern is recovered within 1 s (Figure 2d). The diffraction pattern is recovered with the same orientation every time the field is turned on again.

The evolution of the diffraction pattern indicates that two stages are involved in the assembly of the colloidal crystal. The local dynamics of the particles during these two stages was observed directly using high-magnification optical microscopy (40× or 60× objective). Before the field is applied, it is difficult to obtain a clear image of the particles because they are distributed vertically through the cell and exhibit Brownian motion (Figure 3a). Within 2 s of applying the field, the latex spheres align into chains due to the attractive interactions between the induced dipoles. The chains are parallel to the direction of the applied field and thus are perpendicular to the gap between the two planar electrodes (Figure 3b). As more particle chains collect in the region of maximum field intensity on the surface of the slide, lateral interactions between the chains result in the formation of a hexagonally close-packed 2D array (Figure 3c). It is easy to prove that particle structures such as the ones shown in Figure 3a−c produce the diffraction patterns in Figure 2a−c by simulating the diffraction through digital Fourier transform of the structure in the microscopy images.[43] Thus, the dynamics of chain formation followed by 2D crystallization on the substrate is confirmed by two independent methods, one of which (diffraction) samples the average structure on a large scale, while the other (microscopy) allows one to see it directly on a small scale.

The reflection of a white (polychromatic) beam of light transmitted or reflected at a shallow angle (e.g., 40−80° to normal) was observed using an optical microscope at low magnification. Before the field is applied, only the whitish color of the latex suspension in the cell is visible (Figure 4a). Within seconds of applying the field, a single bright color is seen due to light diffraction by the ordered particle arrays. During the first stage of the process, the appearance of the color depends on the radial angle of the incident light beam. If the light is perpendicular to the direction of the field, no diffracted color appears (Figure 4b), but bright color is observed if the beam is in the direction of the applied field (Figure 4c). This once again confirms the formation of 1D chains of particles that align parallel to the direction of the applied field because such 1D structures diffract only when illuminated in the direction of the chains. Within 10 s after the field is applied, the bright diffraction colors obtained become independent of the direction of the incident light beam (Figure 4d).

(44) Prevo, B. P.; Velev, O. D. *Langmuir*, in press.

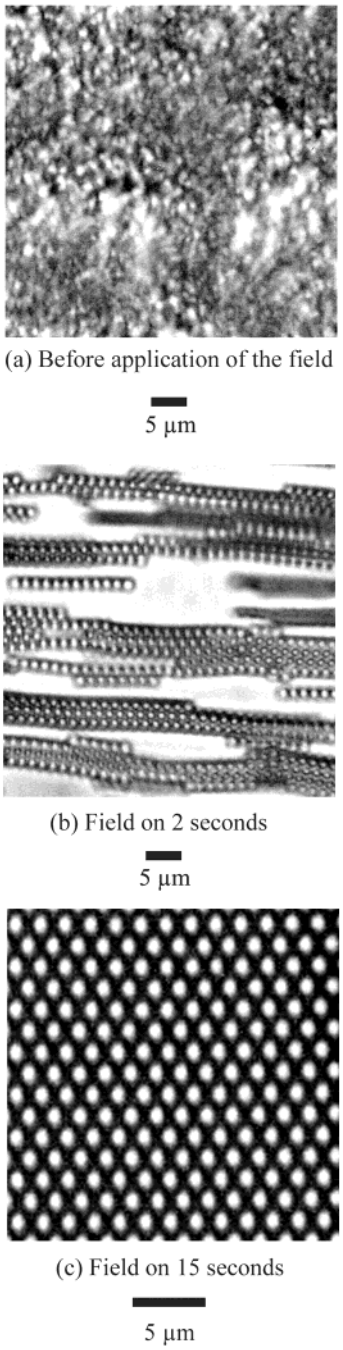

Figure 3. High-magnification images of typical structures observed during the different stages of the crystallization process of 1.4 μm latex particles: (a) random position and Brownian motion before application of the electric field, (b) 1D chains oriented parallel to the direction of the applied field form shortly after the field is applied, and (c) 2D crystal formed due to lateral interaction between chains at longer times. Images a–c correspond to the diffraction patterns shown in Figure 2a–c.

This transition to uniaxial diffraction corresponds to the transition from 1D chains to 2D crystals.

The excellent uniformity of the diffracted color indicates that the particles have aligned into a single periodic crystal throughout the area between the planar electrodes. In this experiment, where the illumination is at a shallow angle, the color arises from diffraction from rows of spheres and is thus dependent on their orientation (similarly to diffraction from line gratings). If multiple smaller domains were formed instead, a much wider range of diffraction

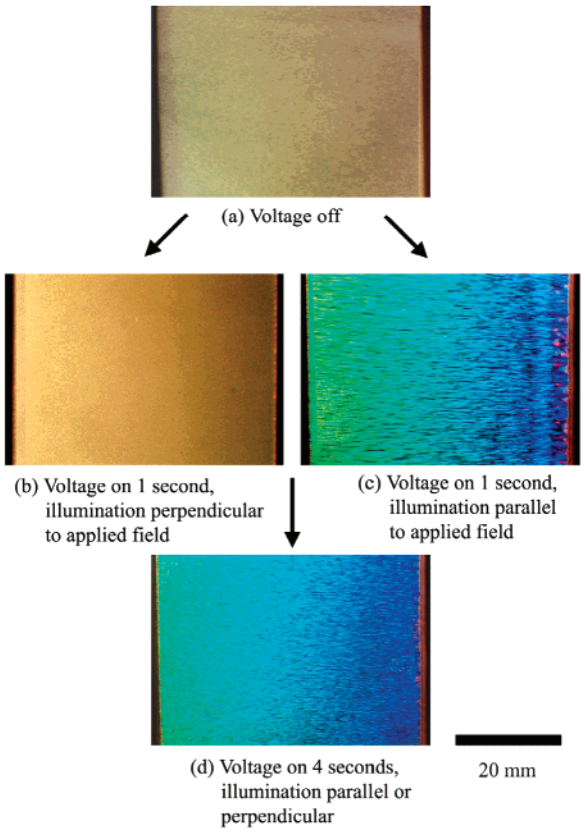

Figure 4. (a) Disordered suspension of particles observed by low-magnification optical microscopy. Intermediate 1D chain formation illuminated from aside with white light perpendicular (b) and parallel (c) to the applied field. (d) Single periodic crystal with uniform color illuminated from any direction.

colors, varying with the orientation of each crystal domain, would be observed. The crystal ultimately consists of a continuous single ordered domain that covers the area of the cell, which is approximately 25 mm^2. This domain size is 2 orders of magnitude larger than that of crystals formed by electrostatic repulsion or by convective assembly onto solid surfaces. The microscopic observation of a single domain is consistent with the single-crystal diffraction obtained anywhere in the cell area. The crystal also has a specific orientation, with one axis aligned parallel to the direction of the applied field. The crystal contains some defects due to impurities or to scratches on the cell, and there are some vacant areas if the particle concentration is not enough to form a complete monolayer, but the sharp and reproducible diffraction pattern demonstrates that the majority of the crystal is free from imperfections and is well-aligned. Crystals of the same orientation are assembled every time the field is reapplied.

Mechanism of Crystal Assembly. Crystal assembly can be readily explained in terms of a combination of the two types of AC-field-driven forces introduced above. Schematics of the two stages of the process are presented in Figure 5. The first, faster stage is the formation of particle chains because of attractive dipolar interparticle interactions (eq 3). This particle chaining is similar to the chain formation process observed in three-dimensional electrorheological fluids.[38,39] However, unlike the situation for oil-based electrorheological suspensions, the aqueous environment and low frequencies used here shift the main source of particle polarizability to the ionic atmosphere, and thus the operating voltages and assembly times are orders of magnitude smaller than typical for electrorheology structure formation in an oil medium.

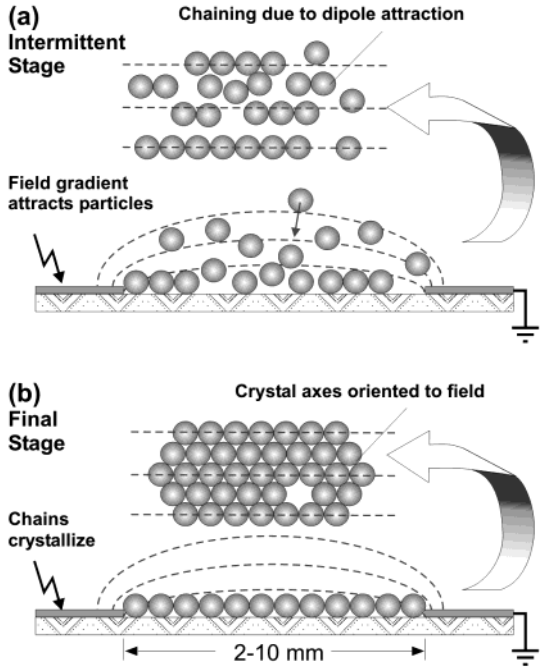

Figure 5. Schematics of the two-stage mechanism of crystallization deduced from the set of diffraction and microscopy data. (a) Immediately after the field is applied, the particles align in chains due to the induced dipole−dipole interactions. Simultaneously, the gradient-driven DEP force pulls the chains and particles toward the surface of the substrate between the electrodes. (b) The particle chains confined on the surface crystallize to form 2D hexagonal crystals aligned by the field.

In the second and slower stage of the crystallization process, the particles and particle chains are attracted to the region of maximum field intensity, which for this geometry is on the surface of the glass slide between the planar electrodes (Figure 5b). The 2D crystal structure then forms on the surface of the slide due to lateral interactions between the dipoles in the adjacent particle chains. This role for the gradient-dependent DEP forces outlines a major difference between the coplanar electrode system studied here and the plane-parallel electrode configurations studied previously.[14−18,39] Hypothetically, the particles can accumulate on the surface by gravity; however, for polystyrene spheres of the size and density used here this would take much longer than the few seconds required for crystal formation in the presence of the field. The role of the DEP attraction and confinement was verified in experiments in which the cell was rotated 180° so that the electrodes were above the colloidal suspension. In this case, the dielectrophoretic force moves the microspheres upward against gravity and they assemble on the top surface. The kinetics of the assembly process and the diffraction pattern remain unaltered, so the DEP force is the major factor confining particles on the surface.

The combination of dipole−dipole chaining and dipole−field gradient forces also explains the specific orientation of the crystal. The assembly of the particles into 1D chains parallel to the direction of the electric field determines the overall orientation of the crystal formed after the chains are crystallized on the glass surface. This, together with the strong in-plane alignment of the arrays because of DEP attraction, sets all of the geometrical parameters of the crystal, which in turn gives the excellent alignment and the consistently predictable position of the diffraction spots.

The process of 2D crystal disassembly in less than a second is remarkably fast compared to the slow relaxation of the structure in most 3D crystals. Disassembly is driven by the Brownian motion of the particles after they are released by the field and accords with diffusion perpendicular to the plane of the substrate, in which direction the particles are not constrained by others in the 2D crystal. Precise calculations of the relaxation times of this process are complex, because they need to take into account the opposing forces of diffusion and gravitational sedimentation. The relative importance of the Brownian and gravitational forces to the particle flux can be evaluated by the Peclet number $Pe = hU/D$, where h is the characteristic displacement (assumed to be on the order of the particle diameter), U is the sedimentation velocity, and D is the particle diffusion coefficient.[45] The sedimentation velocity and diffusion coefficient of a particle of radius r are given by $U = 2\Delta\rho g r^2/9\mu$ and $D = kT/6\pi\mu r$, where $\Delta\rho$ is the difference in the densities, g is the gravitational acceleration, μ is the viscosity, and kT is the Boltzmann constant multiplied by the temperature.

For the latex microspheres studied here, $Pe \approx 0.1$, which means that the random displacement due to thermal forces is only weakly opposed by sedimentation. The length of displacement in the initial stages of Brownian diffusion in the vertical direction can then be estimated by the Einstein−Smoluchowski equation $\langle x^2\rangle^{1/2} = (2Dt)^{1/2}$. The estimated mean square displacement of a 1 μm sphere during the experimentally observed relaxation time of 1 s is 0.9 μm; that is, 1 s is sufficient time for a particle to diffuse far enough to degrade the diffraction pattern. The small Peclet number and corresponding fast relaxation provide yet another proof that the major source of confinement on the surface is the dielectrophoresis, as they prove that gravity alone is not capable of holding these particles in a two-dimensional array.

Effect of Particle Type. To explore the effect of the type of particle on the crystallization process, experiments were made using 1.0 μm silica particles. The same sequence of phenomena was observed, but with different relaxation times. Again, intense diffraction colors are observed in the cell when the 2D crystal is assembled and the diffraction of the laser beam directed through the cell has a similar pattern and evolution (Figure 6). The time taken to form the six-spot diffraction pattern is similar to that for latex particles, which confirms that the forces leading to the 2D crystallization of silica particles are of the same order of magnitude as for the polymer particles. Indeed, the surface charge densities of both types of microspheres are similar, which means that the counterion concentrations and resulting polarization will also be similar.

The relaxation from the ordered arrays to disordered suspension for the silica microspheres, however, was significantly slower than for latex (Figure 6d). This can be explained by the effect of the sedimentation opposing the diffusion-driven disassembly. Due to the higher density of the silica microspheres, the Peclet number of this process is ≈1, that is, 10 times higher than that of similar polystyrene microspheres. This means that there is a significant sedimentation force acting against the Brownian diffusion. The denser silica will take longer to disperse vertically and the crystal will disperse more slowly, in accordance with the experimental observations.

Effect of Particle Size and Electrolyte Concentration. As expected for scattering from hexagonally close-

(45) Russel, W. B.; Saville, D. A.; Schowalter, W. R. *Colloidal Dispersions*; Cambridge University Press: Cambridge, 1999.

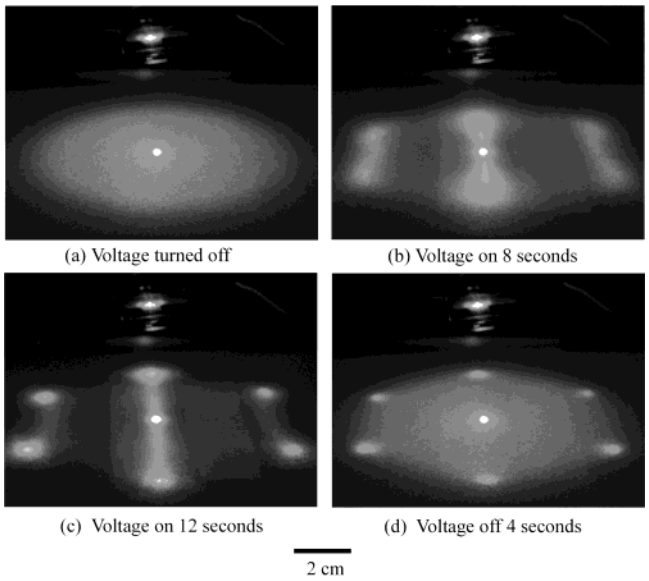

Figure 6. Diffraction pattern obtained from 1 μm silica particles in water as a function of time since application of electric field: (a) before the field is applied, (b) after 8 s, (c) after 12 s applied field, and (d) 4 s after removing the field. Note that the relaxation time after the voltage is turned off is much longer than for latex, comparing image d with Figure 2d.

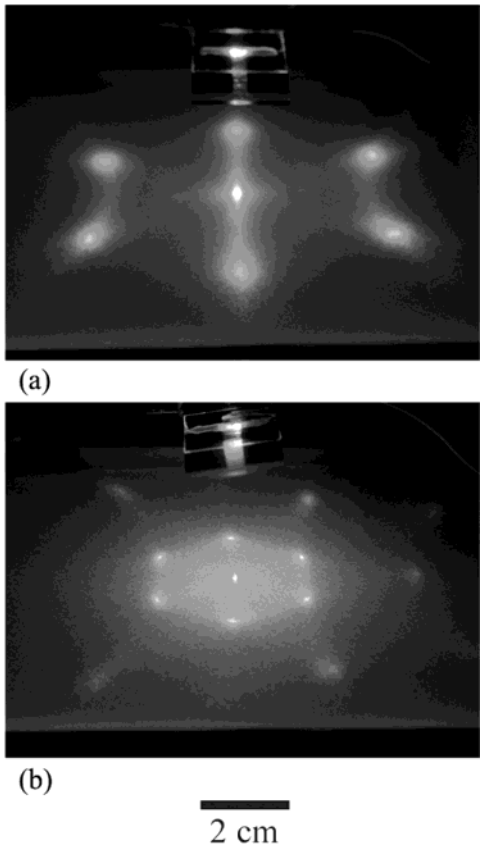

Figure 7. Diffraction patterns from aligned suspensions of (a) 0.7 μm and (b) 1.4 μm latex microspheres. Note the clearly visible second-order diffraction spots in image b.

packed spheres, the angle of diffraction depends on the size of the particles in the array (Figure 7). The diffraction angle (θ) in scattering from a 2D array is related to the lattice spacing (h) via the von Laue equation:

$$h = \frac{n\lambda_c}{\sin\theta} \tag{4}$$

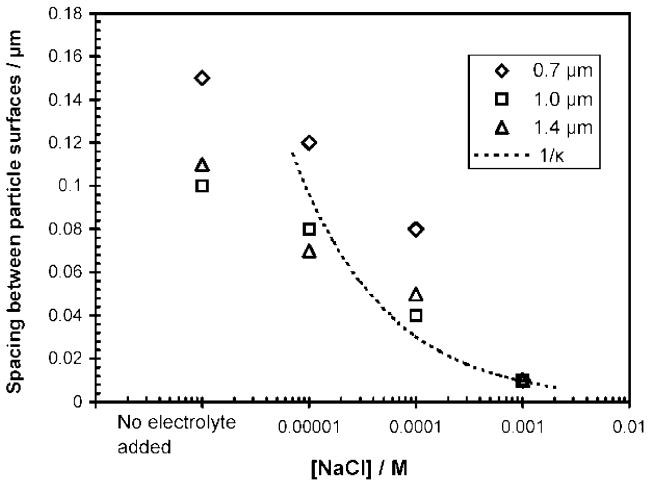

Figure 8. The effect of added electrolyte on the closest distance between particle surfaces calculated from the diffraction angle.

where n is an integer equal to 1 for the diffraction spots nearest to the beam, and λ_c is the wavelength of the laser beam corrected for the refractive indices of the composite media in the scattering environment. λ_c is calculated from the wavelength of the laser in air, λ_0, and the composite refractive index of the media:[46]

$$\lambda_c = \frac{\lambda_o}{(\phi n_p^2 + (1-\phi)n_w^2)^{1/2}} \tag{5}$$

where ϕ is the volume fraction of particles in a monolayer, and n_p and n_w are the refractive indices of latex particles and water, respectively. The diffraction angle is also corrected for refraction of the laser beam as it exits the cell using Snell's law. Subtracting the particle diameter from the calculated center-to-center spacing yields the distance between the surfaces of the particles, and this distance depends on the concentration of electrolyte in the aqueous phase (Figure 8). In pure water, the measured distance between particle surfaces is approximately 10−15% of the particle diameter. This is due to repulsive electrostatic interactions between the negatively charged sulfate groups on the latex surfaces. As the concentration of electrolyte in the surrounding media is increased, these interactions are suppressed, and in the presence of 10^{-3} M NaCl the particles are almost in complete contact.

Exact calculations of the effect of electrolyte are complex and require additional data on particle charge as a function of electrolyte and electric potential. However, the distances between the particle surfaces could be expected to be comparable to the Debye length of the counterionic atmosphere, $1/\kappa$.[47] The Debye lengths for the systems with added electrolyte are plotted in Figure 8 (dashed line) and indeed are in a reasonable proximity to the measured data. This control over the repulsive interactions via the electrolyte concentration could be used as a means of fine-tuning the lattice spacing in the crystal. Alternatively, the DEP crystallization method offers a possible way to study long-range multibody particle interactions in ensembles by simple laser diffraction.

Effect of Field Strength and Frequency. The dielectrophoretic response of dielectric microspheres in water depends strongly on the frequency of the applied field (eq 1, refs 22−24), so the crystallization threshold

(46) Pradhan, R. D.; Tarhan, I. I.; Watson, G. H. *Phys. Rev. B* **1996**, *54*, 13721.
(47) Israelachvili, J. N. *Intermolecular and Surface Forces*; Academic Press: London, 1991.

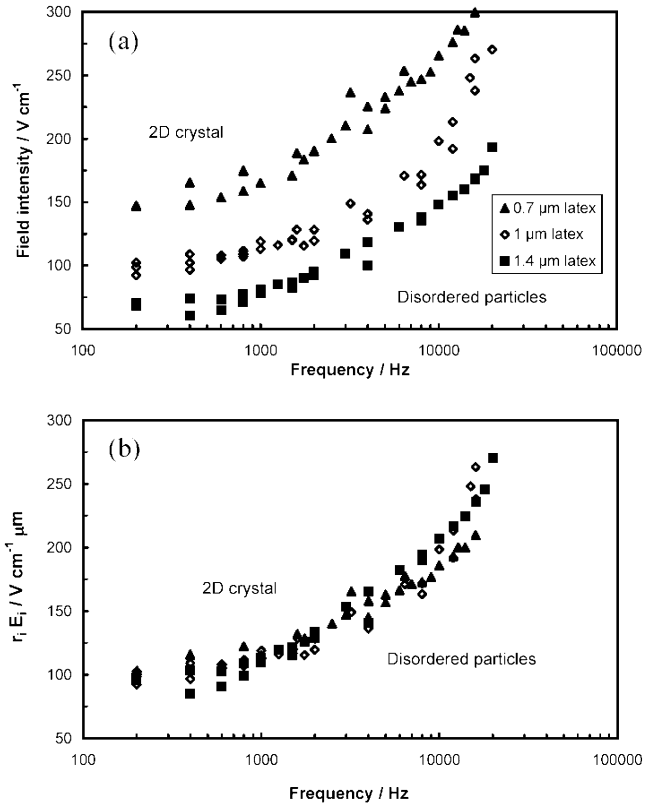

Figure 9. (a) Effect of frequency and particle size on the field intensity required for crystallization for latex microspheres of three diameters (0.7, 1.0, and 1.4 μm). The points for each particle size include data from independent experimental runs. (b) These data are normalized and fall on a single master curve according to predictions of eq 6.

for latex microspheres was explored as a function of the field strength and frequency (Figure 9a). At any particle size, the field strength required to achieve crystallization increases monotonically with the frequency, approximately doubling at the highest frequency studied, 20 kHz. The threshold intensity is lowest at low frequencies and large particle diameters. In principle, particles could be crystallized at even lower voltages and frequencies. This, however, is not practical, as for frequencies below 100 Hz the electrophoretic mobility becomes significant and the particles "vibrate" as they follow the direction of the field electrophoretically. Macroscopic fluid currents also begin to circulate inside the cell at lower frequencies, and these distort the uniformity of the particle layer on the bottom of the cell.

The above data are in good correspondence with the concept of dipolar polarization via displacement of the counterionic atmosphere around the particles. It is important to realize that the latex particles are attracted toward the areas of high field intensity (positive dielectrophoresis) entirely because of the polarizability of the counterionic layer around them. The dielectric permittivity of the bulk material, polystyrene, is much lower than that of water, so the latex particles exhibit negative dielectrophoresis at frequencies above ca. 10^6 Hz, where the counterionic atmosphere cannot respond fast enough to changes in the field. This has been well established experimentally.[25,28] At the relatively low frequencies used in these experiments, however, the ionic polarization effects predominate and the particles are always attracted to the field intensity maximum, which is on the surface of the glass plate near the electrodes. The microspheres

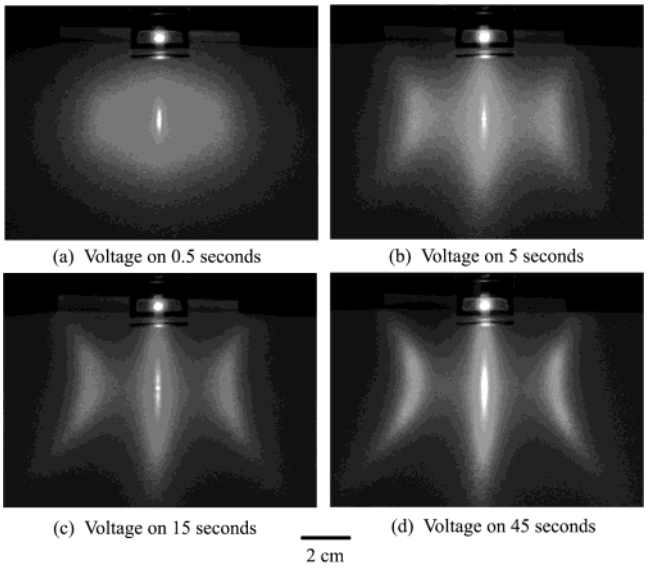

Figure 10. Diffraction patterns obtained from 1.0 μm latex particles in the presence of 40 vol % glycerol as a function of time since application of the electric field: (a) 0.5 s after applying the electric field, (b) 5 s after applying the field, (c) 15 s after applying the field, and (d) 45 s after applying the field. The particles align in chains but do not crystallize in two dimensions.

accumulated on the surface crystallize when the field becomes strong enough.

A few assumptions allow interpretation of the dependence of the threshold voltage on the particle size. At fixed frequency, the intensity required for crystallization increases as the particle diameter decreases (Figure 9a). The first step in the crystallization is the formation of chains via dipolar attraction, so a good assumption is that the process begins only after the chaining force F_{chain} (eq 3) exceeds a certain threshold, $F^{\text{T}}_{\text{chain}}$. Assuming further that $F^{\text{T}}_{\text{chain}}$ depends only weakly on particle size (given that the thermal energy disrupting the array formation is $\approx 3/2\ kT$ per particle regardless of size), eq 3 suggests that

$$\frac{-F^{\text{T}}_{\text{chain}}}{C\pi\epsilon_1 K(\omega)^2} = \text{const} = r_i^2 E_{i,\text{chain}}{}^2 \qquad (6)$$

where $E_{i,\text{chain}}$ is the field strength needed to produce crystals of particles of size r_i. Thus, for any given type of particles and a fixed frequency, the voltage required for crystallization should scale as inversely proportional with particle radius. The measured crystallization threshold data for all three types of particles confirm this hypothesis, yielding a master curve when $r_i E_i$ are plotted as a function of frequency (Figure 9b). This confirms the validity of using the chaining eq 3 in estimating the phase transition threshold, even though at this stage we do not have enough data and theoretical constructs for numerical estimation of the constants C and $K(\omega)$. The crystallization threshold has a relatively weak field dependence on the particle size and shows that at higher field intensities even smaller particles than the ones studied here could be crystallized.

Effect of Media Viscosity and Dielectric Permittivity. The lateral interactions between induced dipoles in the 1D chains can be suppressed by addition of glycerol to the aqueous continuous phase. Figure 10 shows the diffraction pattern obtained from 1 μm latex particles dispersed in 40% glycerol solution. The beam is diffusely scattered by the randomly oriented particles before the field is applied (Figure 10a), and three parallel lines are

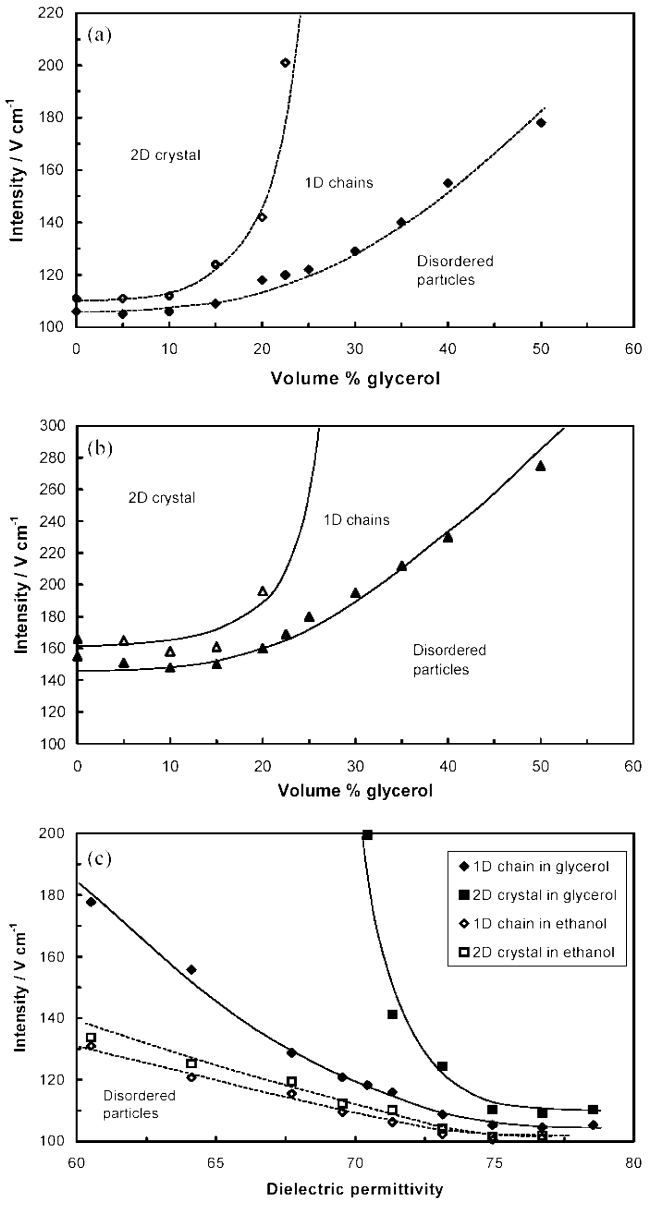

Figure 11. Effect of glycerol concentration on the field intensity required to form 1D chains and 2D crystals at (a) 0.6 kHz and (b) 6 kHz applied frequency. (c) Effect of dielectric permittivity of the continuous phase on chaining and 2D crystal formation (frequency = 0.6 kHz).

observed when the beam is split by the 1D chains (Figure 10b). However, the six-spot diffraction pattern does not appear even after the field is applied for several minutes, so the addition of glycerol to the media in effect opens a new "chain-only" region of the phase transition diagram.

Addition of glycerol to the continuous phase simultaneously increases the viscosity and decreases the dielectric permittivity of the medium. Both could conceivably affect the interactions between the 1D chains of particles. In Figure 11a,b, the field intensity required to assemble 1D chains and 2D crystals is plotted as a function of the concentration of glycerol in the continuous phase at two different frequencies. The filled symbols indicate the intensity required to form 1D chains, and the open symbols show where 2D crystals form. As the concentration of glycerol increases, the field intensity required to form each crystal increases, and above 26 vol % glycerol it is not possible to form 2D crystals at either frequency.

The glycerol effects on viscosity and dielectric permittivity can be separated by carrying out the same experiment with ethanol/water mixtures as the continuous phase. In this case, the dielectric permittivity can be adjusted while maintaining an essentially constant viscosity (Figure 11c). The field intensities required to form 1D chains and 2D crystals in ethanol/water mixtures remain reasonably close, as is the case for water, even at lower values of dielectric permittivity. At the same values of dielectric permittivity, however, it is not possible to form 2D crystals in the presence of glycerol within the intensity range studied. Therefore, medium viscosity plays a key role, perhaps by suppressing counterion mobility and therefore modulating the dipolar and dielectrophoretic interactions. This concept has not yet been developed quantitatively.

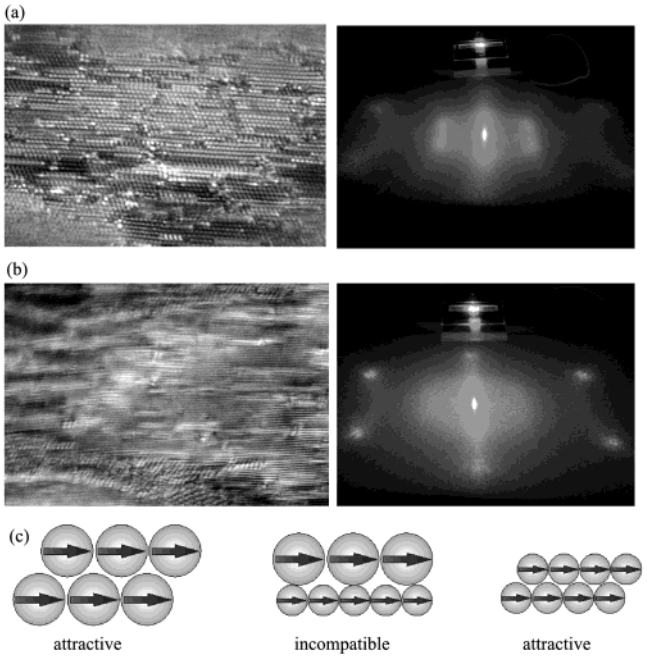

Figure 12. High-magnification optical micrographs (left) and diffraction pattern (right) of the systems assembled from mixtures of 0.7 and 1.4 μm latex particles. (a) Surface fraction of large particles is larger (4:1 large/small particle ratio). (b) Surface fraction of small particles is larger (1:4 large/small particle ratio). (c) Schematic of the hypothesized incompatibility of dipolar interactions between chains of particles of different sizes.

Dielectrophoretic Assembly in Mixtures of Two Types of Particles of Different Sizes. One potential application of DEP-driven assembly can be the cocrystallization or separation of mixtures of particles of different sizes. Both the chaining and dielectrophoretic forces depend on the particle size, so a variety of effects can be expected to have a role in cocrystallization. To evaluate the effect of the field on particle mixtures, suspensions containing both 0.7 and 1.4 μm latex spheres were examined. The overall volume fraction of the spheres was commensurate with the formation of complete mixed monolayers. The particles in these mixed systems were always attracted to and formed close-packed structures on the glass surface between the electrodes. The detailed results, not surprisingly, depend strongly on the ratio of the large to small particles.

The laser beam diffraction pattern and high-magnification optical microscopy images for two distinctly different cases are shown in Figure 12a,b. The process is somewhat similar to an interaction-induced phase separation. At a low concentration of small particles (4:1 ratio of 1.4 μm/0.7 μm, Figure 12a), the 1.4 μm particles form a continuous and aligned 2D array at 40 V. The formation of this 2D

crystal is confirmed by a diffraction pattern at small angles that shows a hexagonal array of six spots at locations similar to those observed previously for 1.4 μm particles alone. The smaller fraction of 0.7 μm particles are confined in small nonaligned pockets within this crystal. When the ratio of small to large particles is inverted, the 0.7 μm particles form a continuous 2D crystal at approximately 70 V but prevent the large particles from crystallizing (Figure 12b). The diffraction pattern for this crystal shows the six spots at a higher diffraction angle, consistent with scattering from 0.7 μm particles.

We hypothesize that the observed separation phenomenon begins when the large particles attract each other and form chains during the initial voltage ramp up. The chain-formation threshold of the large particles will be $^1/_2$ of the voltage for the small particles (as proven by our data in Figure 9 described by eq 6). The small particles likely form chains of their own when the voltage increases further. After these chains are attracted by dielectrophoresis to the surface, they form separate 2D domains. A probable reason for the phase separation of the chains formed in this first stage is the incompatibility of the lateral interactions of the dipoles in the chains of particles of different sizes (Figure 12c). Two chains of dipoles of the same size would exhibit some degree of lateral attraction when the particles form hexagonal arrays, as the average distance between the dipole ends of dissimilar charge would be slightly smaller than the average distance between the dipole ends of similar charge. This is the likely reason for the lateral compression and crystallization observed at the second stage of the process (Figure 5, bottom). On the other hand, the interactions between the dipoles in two chains of particles of different sizes are likely to be on average zero as there are no favorable dipolar or shape match configurations along the two chains. Thus, phase separation of the particles would be driven by the size-dependent strength of dipolar interactions and the lack of lateral attraction between chains of dissimilar particles.

This phenomenon is of significant practical importance as it could be used in particle separation processes, where, after field-induced crystal separation, the particles in the discontinuous pockets can be released by lowering the voltage. Alternatively, if the particle diameters are chosen in a way that allows synergistic interactions between particles of different sizes, cocrystallization processes can occur. The formation of lattices of mixed particle sizes is a problem that is not yet solved generally and is of significant interest for making photonic materials.[48] A rich variety of structures may be formed at different sizes, concentrations, and properties of the particles in the mixtures, and this will be a subject of future research.

Conclusions

The use of alternating fields allows rapid and facile manipulation and organization of particles inside colloidal suspensions. The results presented here demonstrate that by using the simple geometry of two electrodes on a surface with a wide gap between them, a variety of ordered phases of microspheres can be assembled. The organization is driven by a combination of two complementary forces arising from the interaction of the dipoles induced in the particles with the field that induces them and interactions between the dipoles themselves. Dipole−dipole interactions lead to chaining and 2D crystallization in hexagonal phases, while the dielectrophoretic force drives the particles toward the surface. The organization of the particles can be conveniently studied by diffraction of a laser beam passing through the thin cell. The alignment of the particle chains along the direction of the field lines produces a clean diffraction pattern that allows investigation of the effect of voltage, frequency, electrolyte concentration, and media viscosity on the ordering processes and on the type of phases formed. The method allows for further elaboration and study of fundamental aspects of the field-driven particle interactions in water for better understanding and control of the origins of the ionic dipolar polarization and its effect on particle mobility and organization. Dielectrophoretic crystallization can also find applications in photonic devices, in particle separations, and in the fabrication of structured materials after developing techniques to permanently immobilize the arrays by photopolymerization or gelation.

Acknowledgment. This study was supported from grants from the National Science Foundation (CTS-9986305 and CTS-0238636) and the Camille and Henry Dreyfus Foundation. We benefited from useful discussions with A. M. Lenhoff and N. J. Wagner.

LA035812Y

(48) Ristenpart, W. D.; Aksay, I. A.; Saville, D. A. *Phys. Rev. Lett.* **2003**, *90*, 128303.